NMRF/TR/09/2020

TECNICAL REPORT

Generation of atmospheric fluxes from NCMRWF GFS based system for Ocean State forecast

Johny C J and V S Prasad

October 2020

National Centre for Medium Range Weather Forecasting
Ministry of Earth Sciences, Government of India
A-50, Sector-62, Noida-201 309, INDIA

Generation of atmospheric fluxes from NCMRWF GFS based system for Ocean State forecast

Johny C J and V S Prasad

October 2020

National Centre for Medium Range Weather Forecasting
Ministry of Earth Sciences
A-50, Sector-62, Noida-201309, INDIA

1	Name of the institute	National Centre for Medium Range Weather Forecasting
2	Document Number	NMRF/TR/09/2020
3	Date of Publication	October 2020
4	Title of the Document	Generation of atmospheric fluxes from NCMRWF GFS based system for Ocean State forecast
5	Type of Document	Technical Report
6	No. Of Pages, Figures and Tables	33 Pages, 5 Figures and 1 Table
7	Number of references	7
6	Author(S)	Johny C J and V S Prasad
7	Originating Unit	NCMRWF
8	Abstract	Report summarizes the generation of surface fluxes from GFS based modelling system at NCMRWF in providing atmospheric forcing to ocean state forecast of INCOIS. Operational GFS model at NCMRWF employs a hybrid assimilation system with a T1534 deterministic forecast and 80 member T574 ensembles. Atmospheric surface fluxes from the deterministic model are generated at two different resolutions 0.125 ° and 0.25 ° and fluxes from ensemble model at 0.25 ° resolution. Atmospheric forcing from the GFS deterministic model and 80 member ensembles are used by INCOIS in running their ocean analysis systems GODAS and HOOFS respectively. The post-processing system of GFS forecasts at NCMRWF with NCEP_POST is discussed and guidance in modifying the system is provided.
9	Security classification	Non-Secure
10	Distribution	Unrestricted distribution
11	Key words	GFS, Ocean state forecast, Atmospheric flux, NCMRWF

Table of Contents

S.I. No.	Topic	Page No.
1	Abstract	5
2	Introduction	6
3	Surface flux generation	8
4	Post processing of model forecasts	9
5	Control XML files	10
6	Conclusion	11
7	References	11
8	Appendix 1	18
9	Appendix 2	19
10	Appendix 3	21

Abstract

Report summarizes the generation of surface fluxes from GFS based modelling system at NCMRWF in providing atmospheric forcing to ocean state forecast of INCOIS. Operational GFS model at NCMRWF employs hybrid assimilation system with a T1534 deterministic forecast and 80 member T574 ensembles. Atmospheric surface fluxes from the deterministic model are generated at two different resolutions 0.125 ° and 0.25 ° and fluxes from ensemble model at 0.25 ° resolution. Atmospheric forcing from the GFS deterministic model and 80 member ensembles are used by INCOIS in running their ocean analysis systems GODAS and HOOFS respectively. The post-processing system of GFS forecasts at NCMRWF using NCEP_POST is discussed and guidance in modifying the system is provided.

Generation of atmospheric fluxes from NCMRWF GFS based system for Ocean State forecast

1. Introduction

GFS model analysis is created at NCMRWF routinely four times a day corresponds to 00, 06, 12, and 18 UTC and, this analysis is used by IMD in providing operational forecasts. At present GFS model version 14.1.0 is used at NCMRWF and produces output in Gaussian grid binary files in NOAA Environmental Modelling System (NEMS) format at T1534L64 resolution. Hybrid 4D Ensemble Var data assimilation system employed in the NCMRWF GFS (NGFS) model uses 80 member T574L64 ensembles for computing flow-dependent background error covariance. Details of the operational NGFS model can be seen in Johny and Prasad (2020). Surface fluxes from GFS (deterministic) model and 80 member ensembles are generated routinely for use in ocean models of Indian National Centre for Ocean Information Services (INCOIS), Hyderabad as atmospheric forcing. Surface fluxes from the GFS system are used by INCOIS in their global ocean data assimilation system (GODAS) and fluxes from ensembles in High-Resolution Operational Ocean Forecast and Reanalysis System (HOOFS) in analysis mode (Francis et al., 2020). Regional Analysis of Indian Ocean (RAIN) is an ensemble-based ocean data assimilation system that uses atmospheric forcing from 80 GFS ensembles and provides the initial condition for HOOFS. INCOIS GODAS analysis provides ocean state initial conditions (I.C.) for the coupled model forecasts using the climate forecast system (CFS) in extended and seasonal scales. NGFS model provides atmospheric initial conditions for the CFS. It is reported that INCOIS GODAS based ocean initial conditions improved CFS forecast over the Indian region compared to National Centers for Environmental prediction (NCEP) GODAS based ocean initial conditions (Rao et al., 2020). Figure 1 depicts the role of NCMRWF GFS system in the ocean analysis system at INCOIS and CFS system at Indian Institute of Tropical Meteorology (IITM), Pune. Accurate information of surface atmospheric fluxes is important in the performance of the ocean models. GFS deterministic model surface fluxes are generated at two different resolutions 0.125 ° and 0.25 ° and ensembles at 0.25 ° resolution. Post-processing of

model analysis and short forecasts corresponds to 00, 06, 12, and 18 UTC is performed priorly in creating required atmospheric fluxes.

NCMRWF is providing operational global forecasts since 1994 using NCEP GFS based global assimilation and forecast systems. Hierarchical development activities in GFS based system in the centre since inception to the year 2011, until the implementation of the T574 hybrid 3D Var assimilation system is discussed in Prasad et al. (2011). The upgraded NGFS system provided good improvement in model forecast skills and used by other organizations for ocean state forecasts and seasonal forecasting over the Indian region. Operational NGFS model assimilation system upgraded from 3D Var to Hybrid 3D Ensemble Var in 2016 January with a deterministic model of T574 resolution and 80 member T254 EnKF ensembles. In the EnKF system ensemble square root filter is employed for generating ensembles. In the hybrid configuration model uncertainty is estimated by combining flow-dependent error covariance computed using short forecast from ensembles and static error covariance computed using the NMC method. In that hybrid system, 0.75 weight is given to ensemble error covariance and 0.25 weight is given to static error covariance. Hybrid system improved the forecast over 3D Var in temperature, wind, humidity, and rainfall. Improvement is seen in the simulation of extreme rainfall events also. The details of the implementation of the Hybrid Gridpoint statistical interpolation (GSI) system can be seen in Prasad et al. (2016). Hybrid system upgraded to a deterministic model of T1534 (~13km) resolution with semi-Lagrangian dynamics and 80 member EnKF ensembles of T574 resolution in June 2016. In the new hybrid system, 0.875 weight is given to ensemble error covariance and 0.125 weight is given to static error covariance. System upgraded to Hybrid 4D Ensemble Var which uses hourly ensemble forecasts as time-varying background error covariance instead of expensive tangent linear and adjoint model as used in 4D Var formulations in April 2017. A variational bias correction to aircraft temperatures and all-sky assimilation introduced in GSI with the assimilation of AMSUA satellite data. Land surface characteristics for grassland and cropland in the land surface model Noah LSM were changed to reduce summertime warm and dry biases over the Great Plains; convective gravity wave drag was updated. Hybrid system adopted NEMS configuration in 2018 which provides forecasts in the native grid. This implementation introduced the use of near-surface sea Temperature (NSST) and modifications in the cumulus convection scheme and Land surface. MODIS based land surface albedo, 1 km resolution 20 type MODIS IGBP vegetation and

National Cooperative Soil Survey and supersedes the State Soil Geographic (STATSGO) soil climatology replaced older 1° climatology. An additional stability parameter constraint is introduced to prevent the land-atmosphere system from fully decoupling. Before the change, decoupling sometimes produced excessive near-surface cooling in the late afternoon and night time that persisted for hours. The stability constraint improved 2-m air temperature forecasts, temperature forecasts throughout the lower atmosphere and forecasts of light and medium amounts of precipitation. New scale-aware mass-flux shallow convection scheme modified the existing mass-flux shallow convection scheme by introducing the effect of aerosol and information of model resolution (White et al., 2018). NSST provides information of the diurnal cycle of the temperature structure at the ocean surface due to diurnal warming and sub-layer cooling. NSST supplies SST to the atmospheric model for the calculation of air-sea heat and moisture fluxes and providing a sub-layer temperature profile forecast for use as a first guess in the assimilation of SST. Currently, this system utilizes many Indian observations like INSAT3DR, IMD GPSIPW, SAPHIR, SCATSAT along with other global observations.

Details of various steps involved in the model run are described in the previous reports and only major changes are presented here. The steps involved in the deterministic part of the model are the same as discussed in Prasad et al. (2011) except an additional step of preparing blended sea ice analysis and snow analysis. The ensemble section of the model involve steps like select, innovate, update, recentre, forecast, and post. The select step involves the selection of observations from GSI analysis to ensembles and computation of innovations with respect to background ensemble mean. The innovate step does the computation of innovations with respect to each ensemble member background. The update step does assimilation of observations to the ensemble system using the ensemble square root filter technique utilizing innovations computed in the previous two steps. Recentre step recentres each ensemble analysis with respect to deterministic analysis. In the forecast step, a short-range forecast is generated and in post ensemble mean is computed. The flow chart of the hybrid 4D Ensemble Var system is given in Figure 2.

2. Surface flux generation

Surface flux generation involves various steps, post-processing of analysis/forecast outputs, selection of required variables, conversion from Gaussian grid to regular lat/long grid, and

changing the resolution to appropriate dimension at every cycle using the wgrib2 utility. Appendix 1 provides some relevant portions of the codes used in changing resolution and generation of surface fluxes. Figure 3 provides a schematic representation of surface flux generation from deterministic model outputs. Production of the final output to INCOIS is done only at 00 UTC by using appropriate resolution grib2 files generated at 00, 06, 12, and 18 UTC of the previous day and current day 00 UTC. Totally 14 variables are generated for the generation of Ocean State Forecast (OSF) files in the GFS model. Table 1 provide details of fields generated for providing atmospheric forcing to OSFs. In the atmospheric forcing files generated from the deterministic model outputs, 3 hourly average/accumulated fields are used. In addition to variables listed in Table 1, geo-potential height at 500 hPa is also created for OSF flux files from deterministic model outputs.

In the generation of atmospheric flux fields from ensembles, 80 member ensemble forecasts are post-processed and converted to 0.25 ° resolution at every cycle. Final flux output to INCOIS is generated at 00 UTC only combining previous day and current day files as mentioned previously. Here we are post-processing only the required variables for atmospheric fluxes and 6 hourly average/accumulated fields are used. Figure 4 provides a schematic representation of atmospheric flux generation from ensemble outputs.

3. Post processing of model forecasts

NCEP post-processing package NCEP_POST is used to convert model forecast outputs to a more useful grib format (grib1/grib2). It also computes various diagnostic fields from model output variables at different desired pressure levels and different grids. NCEP_POST is a common post-processing platform for all NCEP models and details are provided in the UPP V3: User's Guide. Grib2 output variables are controlled by XML files and grib1 output variables are controlled by "parm" (for example: gfs_cntrl.parm) files. In the present post-processing system at NCMRWF, we are working on grib2 files only. Definitions of the directory structure used in this document are given below.

HOME=/home/gfsprod/
NWPROD=/home/gfsprod/nwprod
log=/scratch/gfsprod/nwwork3/log
rundir574=/home/gfsprod/nwprod/rundirv14_574

parm= home/gfsprod/nwprod/global_shared.v14.1.2/parm

Our post-processing system (entire GFS jobs) follows a particular directory structure in which all PBS scheduler master jobs are kept in the directory “rundir574”. At the submission time, respective PBS scheduler jobs kept in “rundir574” are copied to the “log” directory kept in the system’s scratch area by replacing date and cycle information with appropriate values, and the job is submitted from “log” directory. Figure 5 provides a flow chart of various steps involved in post processing jobs. Two different executables are used for processing forecast fields with 3-hour average/accumulation and 6-hour average/accumulation. The original NCEP_POST code with 6-hour average/accumulation is modified to use it for a 3-hour average/accumulation. The executables and source code are separately available in the “nwprod” directory with the names ncep_post.fd_3hrly and ncep_post.fd_6hrly.

4. Control XML files

Output variables in NCEP_POST are controlled by an XML file (postcntrl_gfs.xml) and post flat files (postxconfig-NT-GFS.txt) kept in the “parm” directory. To modify the output variables first one has to modify the XML file and compile the code to generate a post flat file. NCEP_POST program reads a post flat file to generate the required variables. All the required programs, compilation code (makefile.sh) are available in the “parm” directory. In addition to the XML file mentioned above, there are two more XML files for processing analysis fields (gfs_cntrl.parm_anl) and 00 hr forecasts (postcntrl_gfs_f00.xml). Again, meta-information like originating centre, model details, etc in grib2 files can be altered by modifying XML files. In order to change originating centre to India RSMC/RAFC region, replace the string (<orig_center>nws_ncep</orig_center>) in header information of XML file with the string (<orig_center>new_delhi1</orig_center>) for the centre code 28. To change the centre code to 29 use new_delhi2. Along with this change, some variables require dropping of string “NCEP” in XML file <table_info>NCEP</table_info> for proper naming of the variables. NCEP_POST uses variable information from the WMO table and NCEP local table. In changing the originating centre, the information contained in the WMO table will be displayed without any change in parameter names. Variables names common in both WMO and NCEP table will be displayed properly on removing string <table_info>NCEP</table_info>in XML files. But the variables unique in NCEP local table will be displayed with parameter numbers instead of names with changes in name. To display these variables names an additional local grib table can be

created for these variables with the information of the new originating centre. This local grib table can be compiled along with wgrib2 utility. Alternatively, the grib2 local table of required variables with the changed originating centre is created and can be linked to existing wgrib2 utility. Information on total available variables in NCEP_POST can be obtained from post_avblflds.xml and can use this information to modify the XML files used in the post-processing system. Appendix 2 provides some guidance in modifying XML files. The details of various fields available in the post-processing system NCEP_POST and field definitions are provided in Appendix 3.

5. Conclusion

Ocean surface fluxes are generated from NCMRWF GFS model and 80 member ensembles operationally at different resolutions. The data is utilized by INCOIS in their GODAS and HOOFS ocean analysis system for providing atmospheric forcing.

References

Johny, C. J., and V. S. Prasad, 2020: Application of hind cast in identifying extreme events over India, J. Earth Syst. Sci. 129:163,https://doi.org/10.1007/s12040-020-01435-8.

Francis P. A, Jithin A. K, Effy B. John, Abhisek Chatterjee, Kunal Chakraborty, Arya Paul, Balaji B, S. S. C. Shenoi, Biswamoy P, Arnab Mukherjee, Prerna Singh, Deepsankar B, Siva Reddy S, Vinayachandran P. N, Girish Kumar M. S, Udaya Bhaskar T. V. S, Ravichandran M, Unnikrishnan A. S, Shankar D, Amol Prakash, Aparna S. G, Harikumar R, Kaviyazhaku K, Suprit K, Venkat Shesu R, Kiran Kumar N, Srinivasa Rao N, Annapurnaiah K, Venkatesan R, Suryachandra Rao A, Rajagopal E. N, Prasad V. S, Munmun Das Gupta, Balakirishnan Nair T. M, Pattabhi Rama Rao E, Satyanarayana B. V., 2020: High-resolution Operational Ocean Forecast and reanalysis System 1 for the Indian Ocean, Bulletin of the American Meteorological Society. DOI: 10.1175/BAMS-D-19-0083.1

Rao Suryachandra, A., Goswami, B. N., Sahai, A. K., Rajagopal, E. N., Mukhopadhyay, P., Rajeevan, M., Nayak, S., Rathore, L. S., Shenoi, S. S. C., Ramesh, K. J., Nanjundiah, R., Ravichandran, M., Mitra, A. K., Pai, D. S., Bhowmik, S. K. R., Hazra, A., Mahapatra, S., Saha, S. K., Chaudhari, H. S., Joseph, S., Pentakota, S., Pokhrel, S., Pillai, P. A., Chattopadhyay, R.,

Deshpande M, Krishna, R. P. M., Siddharth Renu, Prasad, V. S., Abhilash, S., Panickal, S., Krishnan, R., Kumar, S., Ramu, D. A., Reddy, S. S., Arora, A., Goswami, T., Rai, A., Srivastava, A., Pradhan, M., Tirkey, S., Ganai, M., Mandal, R., Dey, A., Sarkar, S., Malviya, S., Dhakate, A., Salunke, K. and Maini Parvinder., 2020: Monsoon mission: A targeted activity to improve monsoon prediction across scales. Bull. Am. Meteorol. Soc.100 2509–2532.

Prasad, V. S., Saji Mohandas., Munmundas Gupta, E. N. Rajagopal and Surya Kanti Datta, 2011: Implementation of upgraded global forecasting systems (T382L64 and T574L64) at NCMRWF, NCMR/TR/5/2011.

Prasad, V. S., Johny, C. J., and Jagdeep Singh S. 2016: Impact of 3D Var GSI-ENKF hybrid data assimilation system. J. Earth Syst. Sci. 125(8), 1509–1521. DOI 10.1007/s12040-016-0761-3.

UPP Users' Guide V3.0 available online at
(http://www.dtcenter.org/upp/users/docs/user_guide/V3/upp_users_guide.pdf).

White, G., Yang, F., and Tallapragada, V. 2018: The Development and Success of NCEP's Global Forecast System; National Centers for Environmental Prediction: National Oceanic and Atmospheric Administration, USA

Acknowledgements

Authors are thankful to Head NCMRWF for the support provided in carrying out this work.

Table 1 showing atmospheric flux variables to ocean state forecast

Variables
Total Precipitable Water
Surface Temperature
Temperature at 2m
Specific humidity 2m
U wind 10m
V wind 10 m
Sensible heat flux
Latent heat flux
Downward long wave radiation
Upward long wave radiation
Downward short-wave radiation
Upward short-wave radiation
Precipitation
Mean sea Level pressure

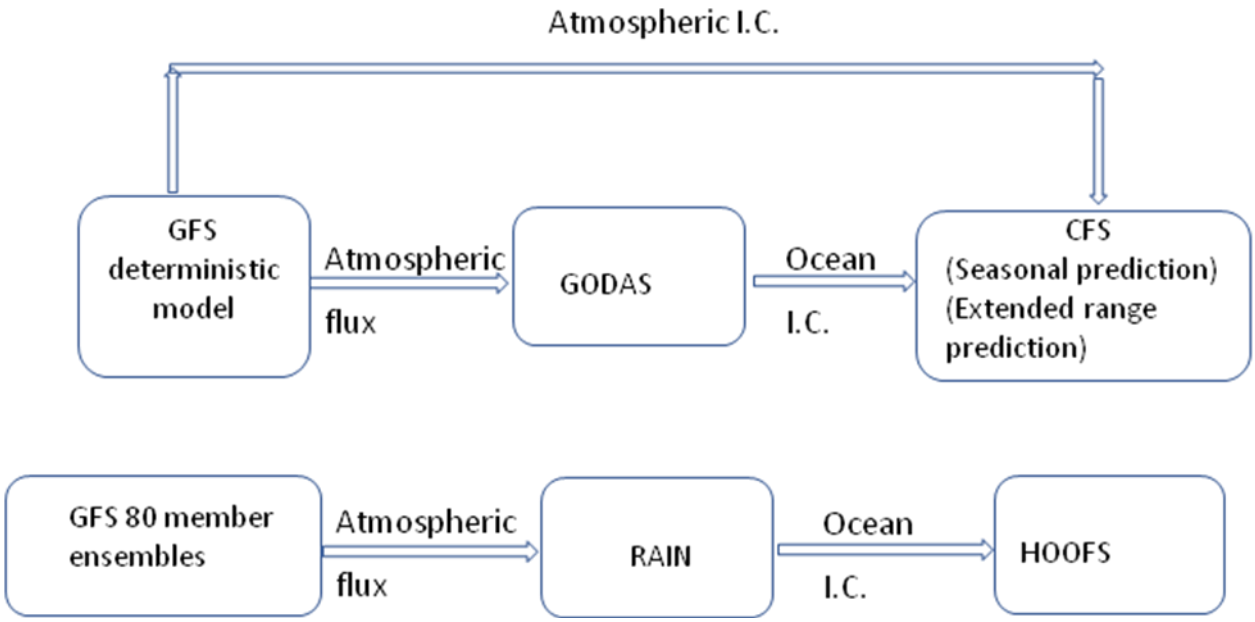

Figure 1 shows the role of atmospheric fluxes from the NCMRWF GFS model in the ocean analysis system at INCOIS and CFS at IITM

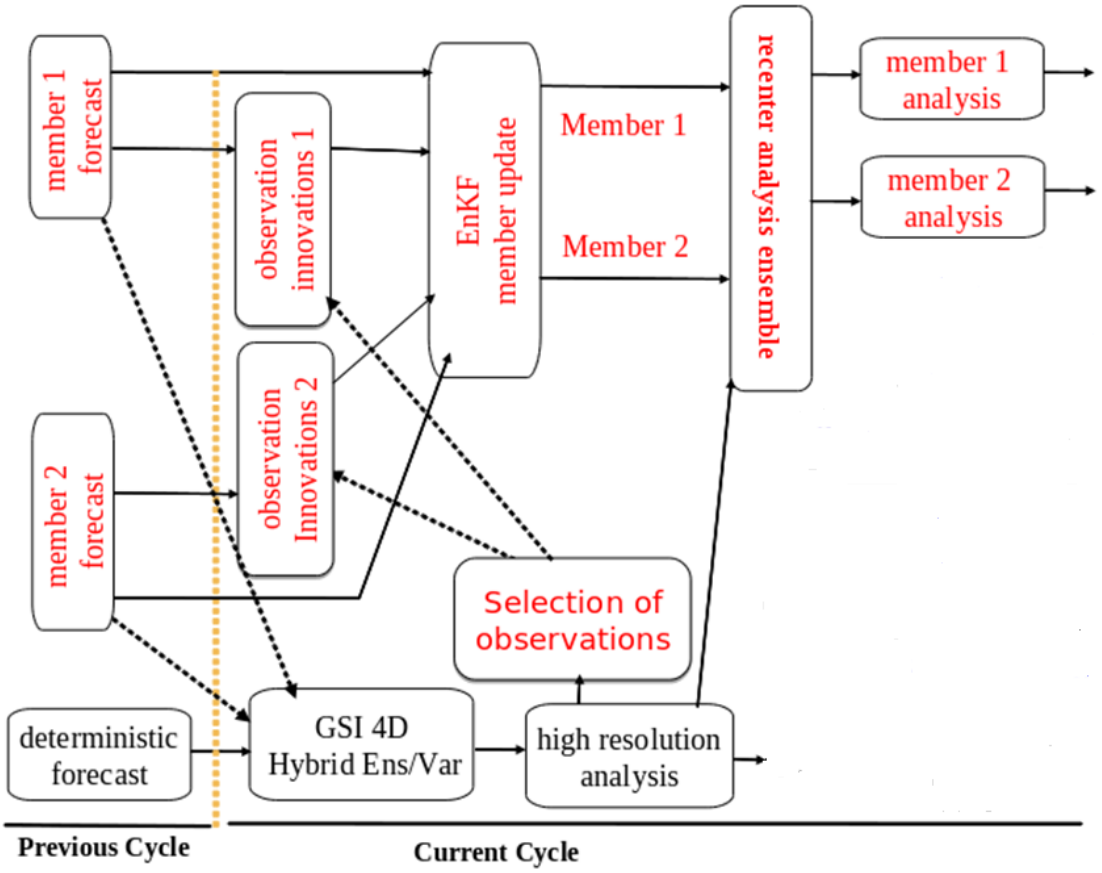

Figure 2 shows Hybrid 4D Ensemble Var GFS modeling system at NCMRWF

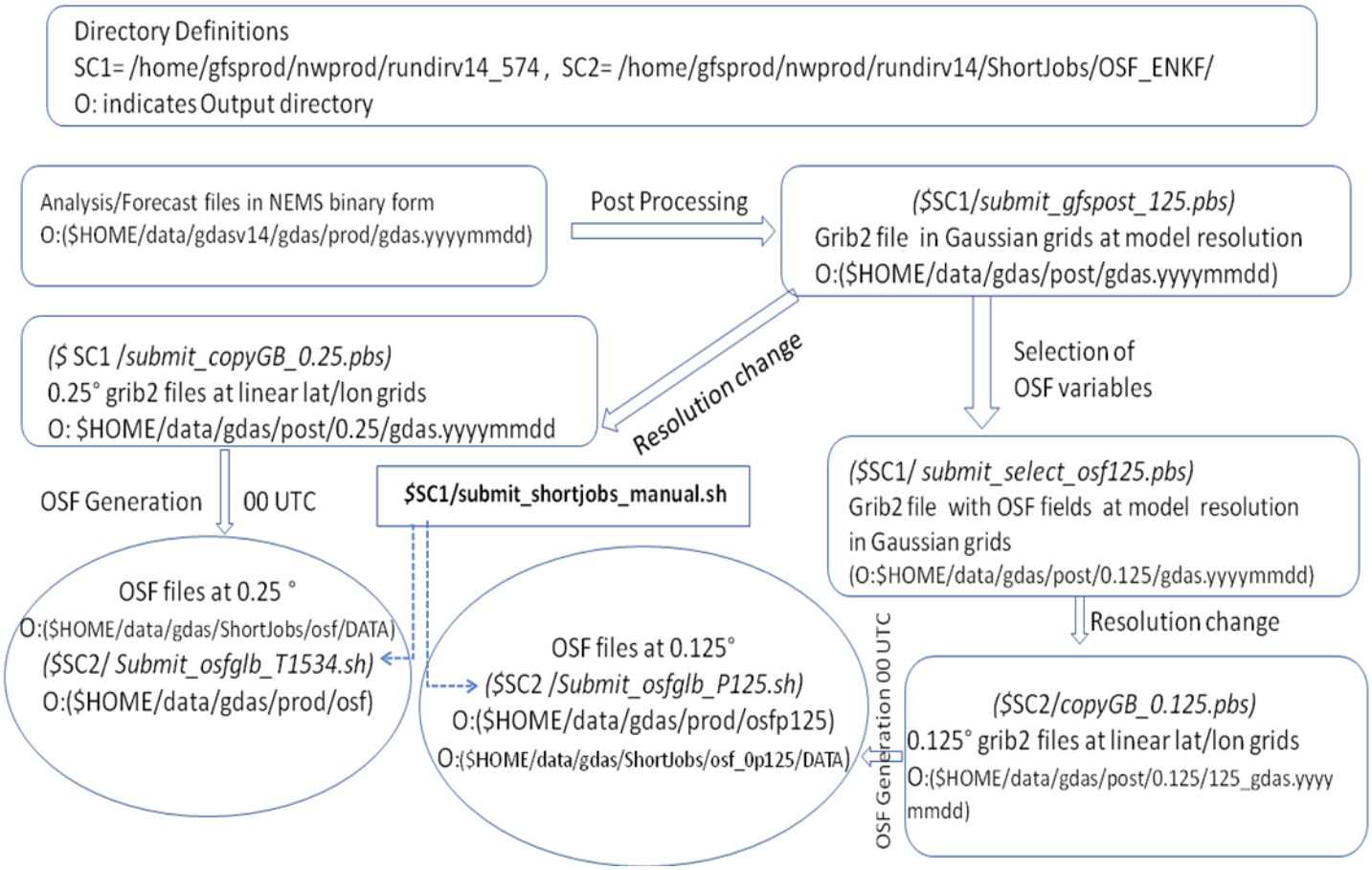

Figure 3 Schematic representation of OSF flux generation from the GFS model deterministic outputs

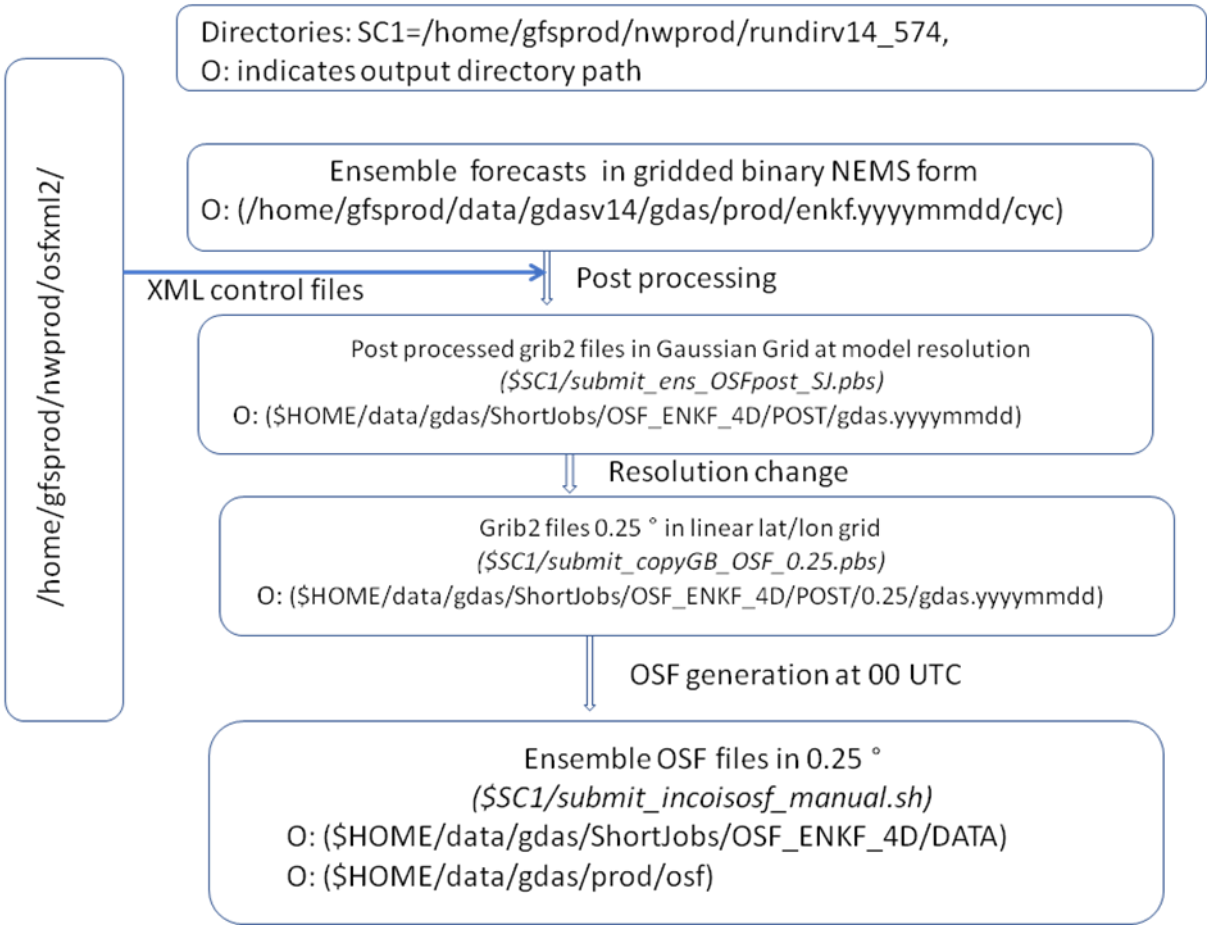

Figure 4 Schematic representation of OSF flux generation from ensemble outputs

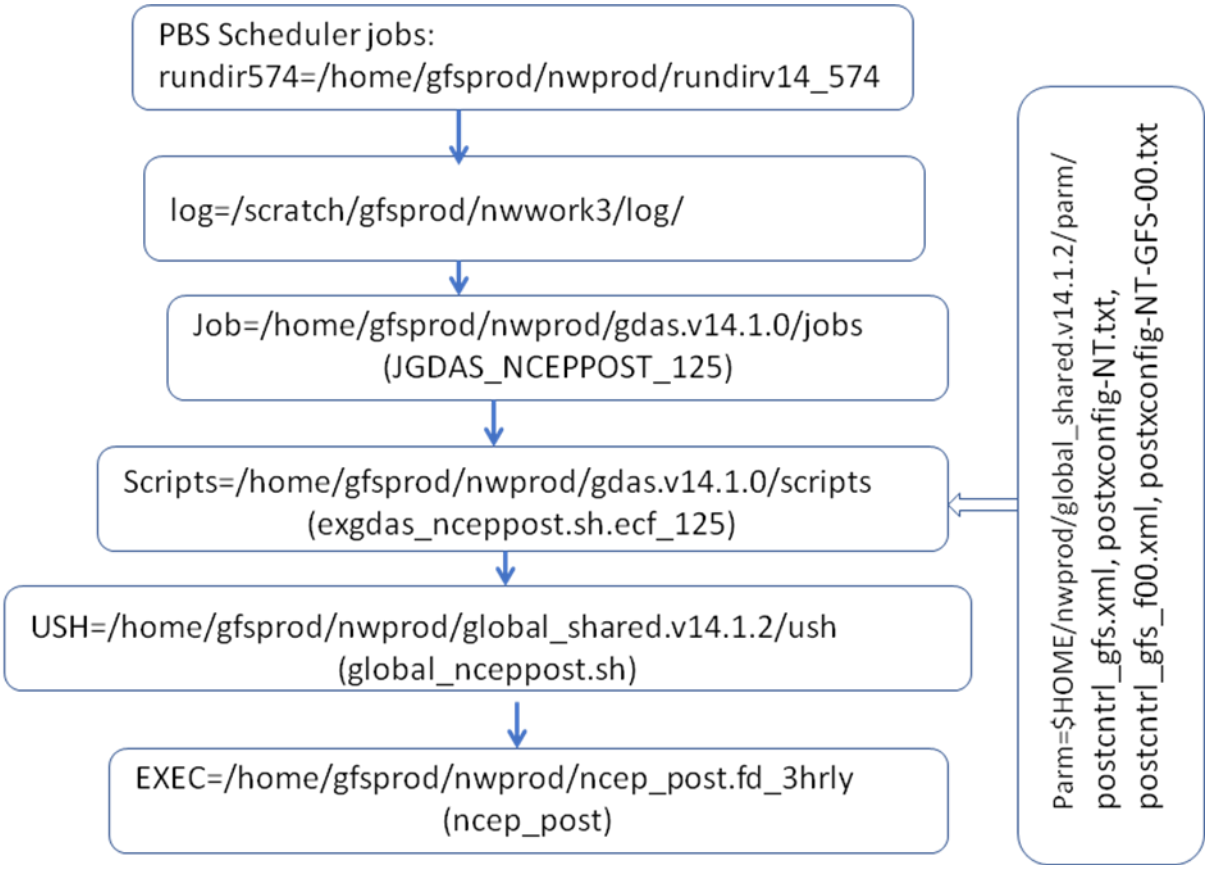

Figure 5 shows the steps involved in the post-processing system at NCMRWF

Appendix 1

Changing the resolution of post processed files to 0.125 degree

```
/home/${LOGNAME}/nwprod/util/exec/wgrib2 $COMIN/gdas1.t${cyc}z.master.grbf$post_times -
new_grid_winds earth -new_gridlatlon 0:2880:0.125 90:1441:-0.125
${COMOUT}/gdas1.t${cyc}z.grbf${post_times}-125
```

Changing the resolution of post processed files to 0.25 degree

```
/home/${LOGNAME}/nwprod/util/exec/wgrib2 $COMIN/gdas.t${cyc}z.master.grb2f$post_times -
new_grid_winds earth -new_gridlatlon 0:1440:0.250 90:721:-0.250
${COMOUT}/gdas1.t${cyc}z.grbf${post_times}-250
```

OSF Flux generation from 0.125 degree files

```
file=$POSTDIR/gdas1.t00z.grbf03-"125"
$wgrib2 $file -s | egrep "(PWAT:entir)"|$wgrib2 -i $file -grib anal_03z-125
$wgrib2 $file -s | egrep "(PRMSL)"|$wgrib2 -i $file -append -grib anal_03z-125
$wgrib2 $file -s | egrep "(TMP:2 m )"|$wgrib2 -i $file -append -grib anal_03z-125
$wgrib2 $file -s | egrep "(SPFH:2 m )"|$wgrib2 -i $file -append -grib anal_03z-125
$wgrib2 $file -s | egrep "(UGRD:10 m )"|$wgrib2 -i $file -append -grib anal_03z-125
$wgrib2 $file -s | egrep "(VGRD:10 m )"|$wgrib2 -i $file -append -grib anal_03z-125
$wgrib2 $file -s | egrep "(SHTFL:surface)"|$wgrib2 -i $file -append -grib anal_03z-125
$wgrib2 $file -s | egrep "(LHTFL:surface)"|$wgrib2 -i $file -append -grib anal_03z-125
$wgrib2 $file -s | egrep "(DLWRF:surface)"|$wgrib2 -i $file -append -grib anal_03z-125
$wgrib2 $file -s | egrep "(ULWRF:surface)"|$wgrib2 -i $file -append -grib anal_03z-125
$wgrib2 $file -s | egrep "(USWRF:surface)"|$wgrib2 -i $file -append -grib anal_03z-125
$wgrib2 $file -s | egrep "(DSWRF:surface)"|$wgrib2 -i $file -append -grib anal_03z-125
$wgrib2 $file -s | egrep "(APCP:surface)"|$wgrib2 -i $file -append -grib anal_03z-125
file=$POSTDIR/gdas1.t00z.grbf03-"125"
$wgrib2 $file -s | egrep "(TMP:surface)"|$wgrib2 -i $file -append -grib anal_03z-125
$wgrib2 $file -s | egrep "(HGT:500 mb)"|$wgrib2 -i $file -append -grib anal_03z-125
```

Changing the originating centre code to 29

```
$HOME/nwprod/util/exec/wgrib2 -set_center 29 anal_03z-125 -grib anal_03z-125a
```

Appendix 2

In order to add a particular field namely“ACM_WEASD_ON_SURFACE” in post processing job.

Corresponding data details in post_avblflds.xml

```
<param>
<post_avblfldidx>35</post_avblfldidx>
<shortname>ACM_WEASD_ON_SURFACE</shortname>
<pdstmpl>tmpl4_8</pdstmpl>
<pname>WEASD</pname>
<stats_proc>ACM</stats_proc>
<fixed_sfc1_type>surface</fixed_sfc1_type>
<scale>4.0</scale>
</param>
```

postcntrl_gfs.xml can be modified for the field like by adding

```
<param>
<shortname>ACM_WEASD_ON_SURFACE</shortname>
<scale>4.0</scale>
</param>
```

Sample local gribtable ‘NCMR_gribtable.dat’ can be used inside wgrib2 programs as below

```
/*
 int disc;   Section 0 Discipline
 int mtab_set;   Section 1 Master Tables Version Number
 int mtab_low;   Section 1 Master Tables Version Number
 int mtab_high;   Section 1 Master Tables Version Number
 int cntr;   Section 1 originating centre, used for local tables
 int ltab;   Section 1 Local Tables Version Number
 int pcat;   Section 4 Template 4.0 Parameter category
 int pnum;   Section 4 Template 4.0 Parameter number
 const char *name;
 const char *desc;
 const char *unit;
*/

{ 0, 1, 0, 255,28, 2, 4, 194, "DUVB", "Direct UV-B Solar Flux", "W m-2"},
{ 0, 1, 0, 255,28, 2, 19, 234, "ICSEV", "Icing severity", "W m-2"},
```

This local gribtable can be included in gribtab.c as shown below and compile the wgrib2 program.

#include "NCMR_gribtable.dat"

Alternatively GRIB2TABLE can be created as below and can be linked with wgrib2 using export command

```
 export GRIB2TABLE=path/filename
/*
  struct gribtable_s {
    int disc;   /* Section 0 Discipline                          */
    int mtab_set;    /* Section 1 Master Tables Version Number used by set_var      */
    int mtab_low;    /* Section 1 Master Tables Version Number low range of tables  */
    int mtab_high;   /* Section 1 Master Tables Version Number high range of tables */
    int cntr;   /* Section 1 originating centre, used for local tables */
    int ltab;   /* Section 1 Local Tables Version Number             */
    int pcat;   /* Section 4 Template 4.0 Parameter category         */
    int pnum;   /* Section 4 Template 4.0 Parameter number           */
    const char *name;
    const char *desc;
    const char *unit;
  };

*/
0:1:0:10:28:1:4:194:DUVB:Direct UV-B Solar Flux: W m-2
0:1:0:10:28:2:19:234:ICSEV:Icing severity:W m-2
```

Appendix 3

Total available fields in NCEP_POST. (GRIB2 fields produced by NCEP_POST(column 1), abbreviated names used in the postcntrl.xml (column 2) and corresponding standard grib2 name (column 3))
(Ref: https://dtcenter.org/sites/default/files/community-code/upp-grib2-table_0.pdf)

Field Description	Name in Grib2 Control File	Grib2 name
Radar reflectivity on model surface	REFD_ON_HYBRID_LVL	REFD
Pressure on model surface	PRES_ON_HYBRID_LVL	PRES
Height on model surface	HGT_ON_HYBRID_LVL	HGT
Temperature on model surface	TMP_ON_HYBRID_LVL	TMP
Potential temperature on model Surface	POT_ON_HYBRID_LVL	POT
Dew point temperature on model Surface	DPT_ON_HYBRID_LVL	DPT
Specific c humidity on model surface	SPFH_ON_HYBRID_LVL	SPFH
Relative humidity on model surface	RH_ON_HYBRID_LVL	RH
Moisture convergence on model surface	MCONV_ON_HYBRID_LVL	MCONV
U component wind on model surface	UGRD_ON_HYBRID_LVL	UGRD
V component wind on model surface	VGRD_ON_HYBRID_LVL	VGRD
Cloud water on model surface	CLWMR_ON_HYBRID_LVL	CLWMR
Cloud ice on model surface	CICE_ON_HYBRID_LVL	CICE
Rain on model surface	RWMR_ON_HYBRID_LVL	RWMR
Snow on model surface	SNMR_ON_HYBRID_LVL	SNMR
Cloud fraction on model surface	TCDC_ON_HYBRID_LVL	TCDC
Omega on model surface	VVEL_ON_HYBRID_LVL	VVEL
Absolute vorticity on model surface	ABSV_ON_HYBRID_LVL	ABSV
Geostrophic streamfunction on model Surface	STRM_ON_HYBRID_LVL	STRM
Turbulent kinetic energy on model Surface	TKE_ON_HYBRID_LVL	TKE
Richardson number on model surface	RI_ON_HYBRID_LVL	RI
Master length scale on model surface	BMIXL_ON_HYBRID_LVL	BMIXL
Asymptotic length scale on model Surface	AMIXL_ON_HYBRID_LVL	AMIXL
Radar reflectivity on pressure surface	REFD_ON_ISOBARIC_SFC	REFD
Height on pressure surface	HGT_ON_ISOBARIC_SFC	HGT
Temperature on pressure surface	TMP_ON_ISOBARIC_SFC	TMP
Potential temperature on pressure Surface	POT_ON_ISOBARIC_SFC	POT
Dew point temperature on pressure Surface	DPT_ON_ISOBARIC_SFC	DPT
Specific humidity on pressure surface	SPFH_ON_ISOBARIC_SFC	SPFH
Relative humidity on pressure surface	RH_ON_ISOBARIC_SFC	RH
Moisture convergence on pressure Surface	MCONV_ON_ISOBARIC_SFC	MCONV
U component wind on pressure surface	UGRD_ON_ISOBARIC_SFC	UGRD
V component wind on pressure surface	VGRD_ON_ISOBARIC_SFC	VGRD
Omega on pressure surface	VVEL_ON_ISOBARIC_SFC	VVEL
Absolute vorticity on pressure surface	ABSV_ON_ISOBARIC_SFC	ABSV

Geostrophic streamfunction on pressure surface	STRM_ON_ISOBARIC_SFC	STRM
Turbulent kinetic energy on pressure Surface	TKE_ON_ISOBARIC_SFC	TKE
Cloud water on pressure surface	CLWMR_ON_ISOBARIC_SFC	CLWMR
Cloud ice on pressure surface	CICE_ON_ISOBARIC_SFC	CICE
Rain on pressure surface	RWMR_ON_ISOBARIC_SFC	RWMR
Snow water on pressure surface	SNMR_ON_ISOBARIC_SFC	SNMR
Total condensate on pressure surface	TCOND_ON_ISOBARIC_SFC	TCOND
Mesinger (Membrane) sea level Pressure	MSLET_ON_MEAN_SEA_LVL	MSLET
Shuell sea level pressure	PRES_ON_MEAN_SEA_LVL	PRMSL
2 M pressure	PRES_ON_SPEC_HGT_LVL_ABOVE_GRND_2m	PRES
2 M temperature	TMP_ON_SPEC_HGT_LVL_ABOVE_GRND_2m	TMP
2 M specific humidity	SPFH_ON_SPEC_HGT_LVL_ABOVE_GRND_2m	SPFH
2 M mixing ratio	Not currently available for grib2	NA
2 M dew point temperature	DPT_ON_SPEC_HGT_LVL_ABOVE_GRND_2m	DPT
2 M RH	RH_ON_SPEC_HGT_LVL_ABOVE_GRND_2m	RH
10 M u component wind	UGRD_ON_SPEC_HGT_LVL_ABOVE_GRND_10m	UGRD
10 M v component wind	VGRD_ON_SPEC_HGT_LVL_ABOVE_GRND_10m	VGRD
10 M potential temperature	POT_ON_SPEC_HGT_LVL_ABOVE_GRND_10m	POT
10 M specific humidity	SPFH_ON_SPEC_HGT_LVL_ABOVE_GRND_10m	SPFH
Surface pressure	PRES_ON_SURFACE	PRES
Terrain height	HGT_ON_SURFACE	HGT
Skin potential temperature	POT_ON_SURFACE	POT
Skin specific humidity	SPFH_ON_SURFACE	SPFH
Skin dew point temperature	DPT_ON_SURFACE	DPT
Skin Relative humidity	RH_ON_SURFACE	RH
Skin temperature	TMP_ON_SURFACE	TMP
Soil temperature at the bottom of soil layers	TSOIL_ON_DEPTH_BEL_LAND_SFC_3m	TSOIL
Soil temperature in between each of soil layers	TSOIL_ON_DEPTH_BEL_LAND_SFC	TSOIL
Soil moisture in between each of soil layers	SOILW_ON_DEPTH_BEL_LAND_SFC	SOILW
Snow water equivalent	WEASD_ON_SURFACE	WEASD
Snow cover in percentage	SNOWC_ON_SURFACE	SNOWC
Heat exchange coefficient at surface	SFEXC_ON_SURFACE	SFEXC
Vegetation cover	VEG_ON_SURFACE	VEG
Soil moisture availability	MSTAV_ON_DEPTH_BEL_LAND_SFC	MSTAV
Ground heat flux - instantaneous	INST_GFLUX_ON_SURFACE	GFLUX
Lifted index surface based	LFTX_ON_ISOBARIC_SFC_500-1000hpa	LFTX
Lifted index best	4LFTX_ON_SPEC_PRES_ABOVE_GRND	4LFTX
Lifted index from boundary layer	PLI_ON_SPEC_PRES_ABOVE_GRND	PLI
CAPE (4 types)	CAPE_ON_SURFACE	CAPE
CIN (4 types)	CIN_ON_SURFACE	CIN
Column integrated precipitable water	PWAT_ON_ENTIRE_ATMOS_SINGLE_LYR	PWAT
Column integrated cloud water	TCOLW_ON_ENTIRE_ATMOS	TCOLW
Column integrated cloud ice	TCOLI_ON_ENTIRE_ATMOS	TCOLI
Column integrated rain	TCOLR_ON_ENTIRE_ATMOS	TCOLR
Column integrated snow	TCOLS_ON_ENTIRE_ATMOS	TCOLS
Column integrated total condensate	TCOLC_ON_ENTIRE_ATMOS	TCOLC

Column integrated cloud water	CWAT_ON_ENTIRE_ATMOS_SINGLE_LYR	CWAT
Helicity	HLCY_ON_SPEC_HGT_LVL_ABOVE_GRND	HLCY
U component storm motion	USTM_ON_SPEC_HGT_LVL_ABOVE_GRND	USTM
V component storm motion	VSTM_ON_SPEC_HGT_LVL_ABOVE_GRND	VSTM
Accumulated total precipitation	ACM_APCP_ON_SURFACE	APCP
Accumulated convective precipitation	ACM_ACPCP_ON_SURFACE	ACPCP
Accumulated grid-scale precipitation	ACM_NCPCP_ON_SURFACE	NCPCP
Accumulated snowfall	ACM_WEASD_ON_SURFACE	WEASD
Accumulated large scale snow	Not currently available for grib2	NA
Accumulated total snow melt	ACM_SNOM_ON_SURFACE	SNOM
Precipitation type (4 types) instantaneous	INST_CRAIN_ON_SURFACE	CRAIN
Precipitation rate - instantaneous	INST_PRATE_ON_SURFACE	PRATE
Composite radar reflectivity	REFC_ON_ENTIRE_ATMOS	REFC
Low level cloud fraction	LCDC_ON_LOW_CLOUD_LYR	LCDC
Mid level cloud fraction	MCDC_ON_MID_CLOUD_LYR	MCDC
High level cloud fraction	HCDC_ON_HIGH_CLOUD_LYR	HCDC
Total cloud fraction	INST_TCDC_ON_ENTIRE_ATMOS	TCDC
Time-averaged total cloud fraction	AVE_TCDC_ON_ENTIRE_ATMOS	TCDC
Time-averaged stratospheric cloud fraction	AVE_CDLYR_ON_ENTIRE_ATMOS	CDLYR
Time-averaged convective cloud fraction	AVE_CDCON_ON_ENTIRE_ATMOS	CDCON
Cloud bottom pressure	PRES_ON_CLOUD_BASE	PRES
Cloud top pressure	PRES_ON_CLOUD_TOP	PRES
Cloud bottom height (above MSL)	HGT_ON_CLOUD_BASE	HGT
Cloud top height (above MSL)	HGT_ON_CLOUD_TOP	HGT
Convective cloud bottom pressure	PRES_ON_CONVECTIVE_CLOUD_BOT_LVL	PRES
Convective cloud top pressure	PRES_ON_CONVECTIVE_CLOUD_TOP_LVL	PRES
Shallow convective cloud bottom pressure	PRES_ON_SHALL_CONVECTIVE_CLOUD_BOT_LVL	PRES
Shallow convective cloud top pressure	PRES_ON_SHALL_CONVECTIVE_CLOUD_TOP_LVL	PRES
Deep convective cloud bottom pressure	PRES_ON_DEEP_CONVECTIVE_CLOUD_BOT_LVL	PRES
Deep convective cloud top pressure	PRES_ON_DEEP_CONVECTIVE_CLOUD_TOP_LVL	PRES
Grid scale cloud bottom pressure	PRES_ON_GRID_SCALE_CLOUD_BOT_LVL	PRES
Grid scale cloud top pressure	PRES_ON_GRID_SCALE_CLOUD_TOP_LVL	PRES
Convective cloud fraction	CDCON_ON_ENTIRE_ATMOS	CDCON
Convective cloud efficiency	CUEFI_ON_ENTIRE_ATMOS_SINGLE_LYR	CUEFI
Above-ground height of LCL	HGT_ON_LVL_OF_ADIAB_COND_FROM_SFC	HGT
Pressure of LCL	PRES_ON_LVL_OF_ADIAB_COND_FROM_SFC	PRES
Cloud top temperature	TMP_ON_CLOUD_TOP	TMP
Temperature tendency from radiative fluxes	TTRAD_ON_HYBRID_LVL	TTRAD
Temperature tendency from shortwave radiative flux	SWHR_ON_HYBRID_LVL	SWHR
Temperature tendency from longwave radiative flux	LWHR_ON_HYBRID_LVL	LWHR
Outgoing surface shortwave radiation - instantaneous	INST_USWRF_ON_SURFACE	USWRF

Outgoing surface longwave radiation - instantaneous	INST_ULWRF_ON_SURFACE	ULWRF
Incoming surface shortwave radiation - time-averaged	AVE_DSWRF_ON_SURFACE	DSWRF
Incoming surface longwave radiation - time-averaged	AVE_DLWRF_ON_SURFACE	DLWRF
Outgoing surface shortwave radiation - time-averaged	AVE_USWRF_ON_SURFACE	USWRF
Outgoing surface longwave radiation - time-averaged	AVE_ULWRF_ON_SURFACE	ULWRF
Outgoing model top shortwave radiation - time-averaged	AVE_USWRF_ON_TOP_OF_ATMOS	USWRF
Outgoing model top longwave radiation - time-averaged	AVE_ULWRF_ON_TOP_OF_ATMOS	ULWRF
Incoming surface shortwave radiation - Instantaneous	INST_DSWRF_ON_SURFACE	DSWRF
Incoming surface longwave radiation - Instantaneous	INST_DLWRF_ON_SURFACE	DLWRF
Roughness length	SFCR_ON_SURFACE	SFCR
Friction velocity	FRICV_ON_SURFACE	FRICV
Surface drag coefficient	CD_ON_SURFACE	CD
Surface u wind stress	UFLX_ON_SURFACE	UFLX
Surface v wind stress	VFLX_ON_SURFACE	VFLX
Surface sensible heat flux - time-averaged	AVE_SHTFL_ON_SURFACE	SHTFL
Ground heat flux - time-averaged	AVE_GFLUX_ON_SURFACE	GFLUX
Surface latent heat flux - time-averaged	AVE_LHTFL_ON_SURFACE	LHTFL
Surface momentum flux - time-averaged	AVE_MFLX_ON_SURFACE	MFLX
Accumulated surface evaporation	ACM_EVP_ON_SURFACE	EVP
Surface sensible heat flux Instantaneous	INST_SHTFL_ON_SURFACE	SHTFL
Surface latent heat flux - Instantaneous	INST_LHTFL_ON_SURFACE	LHTFL
Latitude	NLAT_ON_SURFACE	NLAT
Longitude	ELON_ON_SURFACE	ELON
Land sea mask (land=1 sea=0)	LAND_ON_SURFACE	LAND
Sea ice mask	ICEC_ON_SURFACE	ICEC
Surface midday albedo	ALBDO_ON_SURFACE	ALBDO
Sea surface temperature	WTMP_ON_SURFACE	WTMP
Press at tropopause	PRES_ON_TROPOPAUSE	PRES
Temperature at tropopause	TMP_ON_TROPOPAUSE	TMP
Potential temperature at tropopause	POT_ON_TROPOPAUSE	POT
U wind at tropopause	UGRD_ON_TROPOPAUSE`	UGRD
V wind at tropopause	VGRD_ON_TROPOPAUSE	VGRD
Wind shear at tropopause	VWSH_ON_TROPOPAUSE	VWSH
Height at tropopause	HGT_ON_TROPOPAUSE	HGT
Temperature atflight levels	TMP_ON_SPEC_ALT_ABOVE_MEAN_SEA_LVL	TMP
U wind at flight levels	UGRD_ON_SPEC_ALT_ABOVE_MEAN_SEA_LVL	UGRD
V wind at flight levels	VGRD_ON_SPEC_ALT_ABOVE_MEAN_SEA_LVL	VGRD

Freezing level height (above mean sea level)	HGT_ON_0C_ISOTHERM	HGT
Freezing level RH	RH_ON_0C_ISOTHERM	RH
Highest freezing level height	HGT_ON_HGHST_TROP_FRZ_LVL	HGT
Pressure in boundary layer (30 mb mean)	PRES_ON_SPEC_PRES_ABOVE_GRND	PRES
Temperature in boundary layer (30 mb mean)	TMP_ON_SPEC_PRES_ABOVE_GRND	TMP
Potential temperature in boundary layers (30 mb mean)	POT_ON_SPEC_PRES_ABOVE_GRND	POT
Dew point temperature in boundary layer (30 mb mean)	DPT_ON_SPEC_PRES_ABOVE_GRND	DPT
Specific humidity in boundary layer (30 mb mean)	SPFH_ON_SPEC_PRES_ABOVE_GRND	SPFH
RH in boundary layer (30 mb mean)	RH_ON_SPEC_PRES_ABOVE_GRND	RH
Moisture convergence in boundary layer (30 mb mean)	MCONV_ON_SPEC_PRES_ABOVE_GRND	MCONV
Precipitable water in boundary layer (30 mb mean)	PWAT_ON_SPEC_PRES_ABOVE_GRND	PWAT
U wind in boundary layer (30 mb mean)	UGRD_ON_SPEC_PRES_ABOVE_GRND	UGRD
V wind in boundary layer (30 mb mean)	VGRD_ON_SPEC_PRES_ABOVE_GRND	VGRD
Omega in boundary layer (30 mb mean)	VVEL_ON_SPEC_PRES_ABOVE_GRND	VVEL
Visibility	VIS_ON_SURFACE	VIS
Vegetation type	VGTYP_ON_SURFACE	VGTYP
Soil type	SOTYP_ON_SURFACE	SOTYP
Canopy conductance	CCOND_ON_SURFACE	CCOND
PBL height	HPBL_ON_SURFACE	HPBL
Slope type	SLTYP_ON_SURFACE	SLTYP
Snow depth	SNOD_ON_SURFACE	SNOD
Liquid soil moisture	SOILL_ON_DEPTH_BEL_LAND_SFC	SOILL
Snow free albedo	SNFALB_ON_SURFACE	SNFALB
Maximum snow albedo	MXSALB_ON_SURFACE	MXSALB
Canopy water evaporation	EVCW_ON_SURFACE	EVCW
Direct soil evaporation	EVBS_ON_SURFACE	EVBS
Plant transpiration	TRANS_ON_SURFACE	TRANS
Snow sublimation	SBSNO_ON_SURFACE	SBSNO
Air dry soil moisture	SMDRY_ON_SURFACE	SMDRY
Soil moist porosity	POROS_ON_SURFACE	POROS
Minimum stomatal resistance	RSMIN_ON_SURFACE	RSMIN
Number of root layers	RLYRS_ON_SURFACE	RLYRS
Soil moist wilting point	WILT_ON_SURFACE	WILT
Soil moist reference	SMREF_ON_SURFACE	SMREF
Canopy conductance - solar Component	RCS_ON_SURFACE	RCS
Canopy conductance - temperature Component	RCT_ON_SURFACE	RCT
Canopy conductance - humidity Component	RCQ_ON_SURFACE	RCQ
Canopy conductance - soil component	RCSOL_ON_SURFACE	RCSOL

Potential evaporation	PEVPR_ON_SURFACE	PEVPR
Heat diffusivity on sigma surface	VEDH_ON_SIGMA_LVLS	VEDH
Surface wind gust	GUST_ON_SURFACE	GUST
Convective precipitation rate	CPRAT_ON_SURFACE	CPRAT
Radar reflectivity at certain above ground heights*	REFD_ON_SPEC_HGT_LVL_ABOVE_GRND	REFD
MAPS Sea Level Pressure	MAPS_PRMSL_ON_MEAN_SEA_LVL	PRMSL
Total soil moisture	SOILM_ON_DEPTH_BEL_LAND_SFC	SOILM
Plant canopy surface water	CNWAT_ON_SURFACE	CNWAT
Accumulated storm surface runoff	ACM_SSRUN_ON_SURFACE	SSRUN
Accumulated base flow runoff	ACM_BGRUN_ON_SURFACE	BGRUN
Fraction of frozen precipitation	CPOFP_ON_SURFACE	CPOFP
GSD Cloud Base pressure	Not currently available for grib2	NA
GSD Cloud Top pressure	GSD_PRES_ON_CLOUD_TOP	PRES
Averaged temperature tendency from grid scale latent heat release	AVE_LRGHR_ON_HYBRID_LVL	LRGHR
Averaged temperature tendency from convective latent heat release	AVE_CNVHR_ON_HYBRID_LVL	CNVHR
Average snow phase change heat flux	AVE_SNOHF_ON_SURFACE	SNOHF
Accumulated potential evaporation	ACM_PEVAP_ON_SURFACE	PEVAP
Highest freezing level relative humidity	RH_ON_HGHST_TROP_FRZ_LVL	RH
Maximum wind pressure level	PRES_ON_MAX_WIND	PRES
Maximum wind height	HGT_ON_MAX_WIND	HGT
U-component of maximum wind	UGRD_ON_MAX_WIND	UGRD
V-component of maximum wind	VGRD_ON_MAX_WIND	VGRD
GSD cloud base height	GSD_HGT_ON_CLOUD_BASE	HGT
GSD cloud top height	GSD_HGT_ON_CLOUD_TOP	HGT
GSD visibility	GSD_VIS_ON_CLOUD_TOP	VIS
Wind energy potential	WMIXE_ON_SPEC_HGT_LVL_ABOVE_GRND	WMIXE
U wind at 80 m above ground	UGRD_ON_SPEC_HGT_LVL_ABOVE_GRND	UGRD
V wind at 80 m above ground	VGRD_ON_SPEC_HGT_LVL_ABOVE_GRND	VGRD
Graupel on model surface	GRMR_ON_HYBRID_LVL	GRMR
Graupel on pressure surface	GRMR_ON_ISOBARIC_SFC	GRMR
Maximum updraft helicity	MAX_UPHL_ON_SPEC_HGT_LVL_ABOVE_GRND_2-5km	MXUPHL
Maximum 1km reflectivity	MAX_REF_ON_SPEC_HGT_LVL_ABOVE_GRND_1km	MAXREF
Maximum wind speed at 10m	MAX_WIND_ON_SPEC_HGT_LVL_ABOVE_GRND_10m	WIND
Maximum updraft vertical velocity	MAX_MAXUVV_ON_ISOBARIC_SFC_40-100hpa	MAXUVV
Maximum downdraft vertical velocity	MAX_MAXDVV_ON_ISOBARIC_SFC_40-100hpa	MAXDVV
Mean vertical velocity	AVE_DZDT_ON_SIGMA_LVL_0.5-0.8	DZDT
Radar echo top in KDT	HGT_ON_SPEC_HGT_LVL_ABOVE_GRND	HGT
Updraft helicity	UPHL_ON_SPEC_HGT_LVL_ABOVE_GRND_2-5km	MXUPHL
Column integrated graupel	GRMR_ON_ENTIRE_ATMOS_SINGLE_LYR	GRMR
Column integrated maximum graupel	MAXVIG_ON_ENTIRE_ATMOS_SINGLE_LYR	TCOLG
U-component of 0-1km level wind shear	VUCSH_ON_SPEC_HGT_LVL_ABOVE_GRND_0-1km	VUCSH
V-component of 0-1km level wind shear	VVCSH_ON_SPEC_HGT_LVL_ABOVE_GRND_0-1km	VVCSH

U-component of 0-6km level wind shear	VUCSH_ON_SPEC_HGT_LVL_ABOVE_GRND_0-6km	VUCSH
V-component of 0-6km level wind shear	VVCSH_ON_SPEC_HGT_LVL_ABOVE_GRND_0-6km	VVCSH
Total precipitation accumulated over user-specified bucket	BUCKET_APCP_ON_SURFACE	APCP
Convective precipitation accumulated over user-specified bucket	BUCKET_ACPCP_ON_SURFACE	ACPCP
Grid-scale precipitation accumulated over user-specified bucket	BUCKET_NCPCP_ON_SURFACE	NCPCP
Snow accumulated over user-specified Bucket	BUCKET_WEASD_ON_SURFACE	WEASD
Model level fraction of rain for Ferrier Scheme	FRAIN_ON_HYBRID_LVL	FRAIN
Model level fraction of ice for Ferrier Scheme	FICE_ON_HYBRID_LVL	FICE
Model level riming factor for Ferrier Scheme	RIME_ON_HYBRID_LVL	RIME
Model level total condensate for Ferrier scheme	TCOND_ON_HYBRID_LVL	TCOND
Height of sigma surface	HGT_ON_SIGMA_LVLS	HGT
Temperature on sigma surface	TMP_ON_SIGMA_LVLS	TMP
Specific humidity on sigma surface	SPFH_ON_SIGMA_LVLS	SPFH
U-wind on sigma surface	UGRD_ON_SIGMA_LVLS	UGRD
V-wind on sigma surface	VGRD_ON_SIGMA_LVLS	VGRD
Omega on sigma surface	VVEL_ON_SIGMA_LVLS	VVEL
Cloud water on sigma surface	CLWMR_ON_SIGMA_LVLS	CLWMR
Cloud ice on sigma surface	CICE_ON_SIGMA_LVLS	CICE
Rain on sigma surface	RWMR_ON_SIGMA_LVLS	RWMR
Snow on sigma surface	SNMR_ON_SIGMA_LVLS	SNMR
Condensate on sigma surface	TCOND_ON_SIGMA_LVLS	TCOND
Pressure on sigma surface	PRES_ON_SIGMA_LVLS	PRES
Turbulent kinetic energy on sigma Surface	TKE_ON_SIGMA_LVLS	TKE
Cloud fraction on sigma surface	TCDC_ON_SIGMA_LVLS	TCDC
Graupel on sigma surface	GRLE_ON_SIGMA_LVLS	GRLE
LCL level pressure	PLPL_ON_SPEC_PRES_ABOVE_GRND	PLPL
LOWEST WET BULB ZERO HEIGHT	HGT_ON_LWST_LVL_OF_WET_BULB_ZERO	HGT
Leaf area index	LAI_ON_SURFACE	LAI
Accumulated land surface model Precipitation	ACM_LSPA_ON_SURFACE	LSPA
In- flight icing	TIPD_ON_ISOBARIC_SFC	TIPD
Clear air turbulence	TPFI_ON_ISOBARIC_SFC	TPFI
Wind shear between shelter level and 2000 FT	VWSH_ON_SPEC_HGT_LVL_ABOVE_GRND	VWSH
Ceiling	HGT_ON_CLOUD_CEILING	HGT
Flight restriction	VIS_ON_CLOUD_BASE	VIS
Instantaneous clear sky incoming surface shortwave	INST_CSDSF_ON_SURFACE	CSDSF

Pressure level riming factor for Ferrier Scheme	RIME_ON_ISOBARIC_SFC	RIME
Model level vertical velocity	DZDT_ON_HYBRID_LVL	DZDT
Brightness temperature	SBT122_ON_TOP_OF_ATMOS_FROM_LWRAD	SBT122
Average albedo	AVE_ALBDO_ON_SURFACE	ALBDO
Ozone on model surface	O3MR_ON_HYBRID_LVL	O3MR
Ozone on pressure surface	O3MR_ON_ISOBARIC_SFC	O3MR
Surface zonal momentum flux	AVE_UFLX_ON_SURFACE	UFLX
Surface meridional momentum flux	AVE_VFLX_ON_SURFACE	VFLX
Average precipitation rate	AVE_PRATE_ON_SURFACE	PRATE
Average convective precipitation rate	AVE_CPRAT_ON_SURFACE	CPRAT
Instantaneous outgoing longwave at top of atmosphere	INST_ULWRF_ON_TOP_OF_ATMOS	ULWRF
Total spectrum brightness Temperature	BRTMP_ON_TOP_OF_ATMOS	BRTMP
Model top pressure	PRES_ON_TOP_OF_ATMOS	PRES
Composite rain radar reflectivity	REFZR_ON_ENTIRE_ATMOS	REFZR
Composite ice radar reflectivity	REFZI_ON_ENTIRE_ATMOS	REFZI
Composite radar reflectivity from Convection	REFZC_ON_ENTIRE_ATMOS	REFZC
Rain radar reflecting angle	REFZR_ON_SPEC_HGT_LVL_ABOVE_GRND	REFZR
Ice radar reflecting angle	REFZI_ON_SPEC_HGT_LVL_ABOVE_GRND	REFZI
Convection radar reflecting angle	REFZC_ON_SPEC_HGT_LVL_ABOVE_GRND	REFZC
Model level vertical velocity	DZDT_ON_ISOBARIC_SFC	DZDT
Column integrated super cool liquid Water	TCLSW_ON_ENTIRE_ATMOS	TCLSW
Column integrated melting ice	TCOLM_ON_ENTIRE_ATMOS	TCOLM
Height of lowest level super cool liquid water	HGT_ON_LWST_BOT_LVL_OF_SUPERCOOLED_LIQ_WATER_LYR	HGT
Height of highest level super cool liquid water	HGT_ON_HGHST_TOP_LVL_OF_SUPERCOOLED_LIQ_WATER_LYR	HGT
Richardson number planetary boundary layer height	HGT_ON_PLANETARY_BOUND_LYR	HGT
Total column shortwave temperature Tendency	SWHR_ON_ENTIRE_ATMOS	SWHR
Total column longwave temperature Tendency	LWHR_ON_ENTIRE_ATMOS	LWHR
Total column gridded temperature Tendency	AVE_LRGHR_ON_ENTIRE_ATMOS	LRGHR
Total column convective temperature Tendency	AVE_CNVHR_ON_ENTIRE_ATMOS	CNVHR
Radiative flux temperature tendency on pressure level	TTRAD_ON_ISOBARIC_SFC	TTRAD
Column integrated moisture Convergence	MCONV_ON_ENTIRE_ATMOS	MCONV
Time averaged clear sky incoming UV-B shortwave	AVE_CDUVB_ON_SURFACE	CDUVB
Time averaged incoming UV-B Shortwave	AVE_DUVB_ON_SURFACE	DUVB
Total column ozone	TOZNE_ON_ENTIRE_ATMOS_SINGLE_LYR	TOZNE
Average low cloud fraction	AVE_TCDC_ON_LOW_CLOUD_LYR	TCDC

Average mid cloud fraction	AVE_TCDC_ON_MID_CLOUD_LYR	TCDC
Average high cloud fraction	AVE_TCDC_ON_HIGH_CLOUD_LYR	TCDC
Average low cloud bottom pressure	AVE_PRES_ON_LOW_CLOUD_BOT_LVL	PRES
Average low cloud top pressure	AVE_PRES_ON_LOW_CLOUD_TOP_LVL	PRES
Average low cloud top temperature	AVE_TMP_ON_LOW_CLOUD_TOP_LVL	TMP
Average mid cloud bottom pressure	AVE_PRES_ON_MID_CLOUD_BOT_LVL	PRES
Average mid cloud top pressure	AVE_PRES_ON_MID_CLOUD_TOP_LVL	PRES
Average mid cloud top temperature	AVE_TMP_ON_MID_CLOUD_TOP_LVL	TMP
Average high cloud bottom pressure	AVE_PRES_ON_HIGH_CLOUD_BOT_LVL	PRES
Average high cloud top pressure	AVE_PRES_ON_HIGH_CLOUD_TOP_LVL	PRES
Average high cloud top temperature	AVE_TMP_ON_HIGH_CLOUD_TOP_LVL	TMP
Total column relative humidity	RH_ON_ENTIRE_ATMOS_SINGLE_LYR	RH
Cloud work function	AVE_CWORK_ON_ENTIRE_ATMOS_SINGLE_LYR	CWORK
Temperature at maximum wind level	TMP_ON_MAX_WIND	TMP
Time averaged zonal gravity wave Stress	AVE_U-GWD_ON_SURFACE	U-GWD
Time averaged meridional gravity wave stress	AVE_V-GWD_ON_SURFACE	V-GWD
Average precipitation type	AVE_CRAIN_ON_SURFACE	CRAIN
Simulated GOES 12 channel 2 brightness temperature	SBT122_ON_TOP_OF_ATMOS	SBT122
Simulated GOES 12 channel 3 brightness temperature	SBT123_ON_TOP_OF_ATMOS	SBT123
Simulated GOES 12 channel 4 brightness temperature	SBT124_ON_TOP_OF_ATMOS	SBT124
Simulated GOES 12 channel 5 brightness temperature	SBT126_ON_TOP_OF_ATMOS	SBT126
Cloud fraction on pressure surface	TCDC_ON_ISOBARIC_SFC	TCDC
U-wind on theta surface	UGRD_ON_ISENTROPIC_LVL	UGRD
V-wind on theta surface	VGRD_ON_ISENTROPIC_LVL	VGRD
Temperature on theta surface	TMP_ON_ISENTROPIC_LVL	TMP
Potential vorticity on theta surface	PVORT_ON_ISENTROPIC_LVL	PVORT
Montgomery streamfunction on theta Surface	MNTSF_ON_ISENTROPIC_LVL	MNTSF
Relative humidity on theta surface	RH_ON_ISENTROPIC_LVL	RH
U wind on constant PV surface	UGRD_ON_POT_VORT_SFC	UGRD
V wind on constant PV surface	VGRD_ON_POT_VORT_SFC	VGRD
Temperature on constant PV surface	TMP_ON_POT_VORT_SFC	TMP
Height on constant PV surface	HGT_ON_POT_VORT_SFC	HGT
Pressure on constant PV surface	PRES_ON_POT_VORT_SFC	PRES
Wind shear on constant PV surface	VWSH_ON_POT_VORT_SFC	VWSH
Planetary boundary layer cloud Fraction	AVE_TCDC_ON_BOUND_LYR_CLOUD_LYR	TCDC
Average water runoff	ACM_WATR_ON_SURFACE	WATR
Planetary boundary layer regime	PBLREG_ON_SURFACE	PBLREG
Maximum 2m temperature	MAX_TMAX_ON_SPEC_HGT_LVL_ABOVE_GRND_2m	TMAX
Minimum 2m temperature	MIN_TMIN_ON_SPEC_HGT_LVL_ABOVE_GRND_2m	TMIN
Maximum 2m RH	MAX_MAXRH_ON_SPEC_HGT_LVL_ABOVE_GRND_2m	MAXRH

Minimum 2m RH	MIN_MINRH_ON_SPEC_HGT_LVL_ABOVE_GRND_2m	MINRH
Ice thickness	ICETK_ON_SURFACE	ICETK
Shortwave tendency on pressure surface	SWHR_ON_ISOBARIC_SFC	SWHR
Longwave tendency on pressure surface	LWHR_ON_ISOBARIC_SFC	LWHR
Deep convective tendency on pressure surface	CNVHR_ON_ISOBARIC_SFC	CNVHR
Shallow convective tendency on pressure surface	SHAHR_ON_ISOBARIC_SFC	SHAHR
Grid scale tendency on pressure surface	LRGHR_ON_ISOBARIC_SFC	LRGHR
Deep convective moisture on pressure surface	CNVMR_ON_ISOBARIC_SFC	CNVMR
Shallow convective moisture on pressure surface	SHAMR_ON_ISOBARIC_SFC	SHAMR
Ozone tendency on pressure surface	TOZ_ON_ISOBARIC_SFC	TOZ
Mass weighted potential vorticity	PVMW_ON_ISOBARIC_SFC	PVMW
Simulated GOES 12 channel 3 brightness count	SBC123_ON_TOP_OF_ATMOS	SBC123
Simulated GOES 12 channel 4 brightness count	SBC124_ON_TOP_OF_ATMOS	SBC124
Omega on theta surface	VVEL_ON_ISENTROPIC_LVL	VVEL
Mixing height	MIXHT_ON_SURFACE	MIXHT
Average clear-sky incoming longwave at surface	AVE_CSDLF_ON_SURFACE	CSDLF
Average clear-sky incoming shortwave at surface	AVE_CSDSF_ON_SURFACE	CSDSF
Average clear-sky outgoing longwave at surface	AVE_CSULF_ON_SURFACE	CSULF
Average clear-sky outgoing longwave at top of atmosphere	AVE_CSULF_ON_TOP_OF_ATMOS	CSULF
Average clear-sky outgoing shortwave at surface	AVE_CSUSF_ON_SURFACE	CSUSF
Average clear-sky outgoing shortwave at top of atmosphere	AVE_CSUSF_ON_TOP_OF_ATMOS	CSUSF
Average incoming shortwave at top of atmosphere	AVE_DSWRF_ON_TOP_OF_ATMOS	DSWRF
Transport wind u component	UGRD_ON_PLANETARY_BOUND_LYR	UGRD
Transport wind v component	VGRD_ON_PLANETARY_BOUND_LYR	VGRD
Sunshine duration	SUNSD_ON_SURFACE	SUNSD
Field capacity	FLDCP_ON_SURFACE	FLDCP
ICAO height at maximum wind level	ICAHT_ON_MAX_WIND	ICAHT
ICAO height at tropopause	ICAHT_ON_TROPOPAUSE	ICAHT
Radar echo top	RETOP_ON_ENTIRE_ATMOS_SINGLE_LYR	RETOP
Time averaged surface Visible beam downward solar flux	AVE_VBDSF_ON_SURFACE	VBDSF

Time averaged surface Visible di use downward solar flux	AVE_VDDSF_ON_SURFACE	VDDSF
Time averaged surface Near IR beam downward solar flux	AVE_NBDSF_ON_SURFACE	NBDSF
Time averaged surface Near IR di use downward solar flux	AVE_NDDSF_ON_SURFACE	NDDSF
Average snowfall rate	AVE_SRWEQ_ON_SURFACE	SRWEQ
Dust 1 on pressure surface	DUST1_ON_ISOBARIC_LVL	MASSMR
Dust 2 on pressure surface	DUST2_ON_ISOBARIC_LVL	MASSMR
Dust 3 on pressure surface	DUST3_ON_ISOBARIC_LVL	MASSMR
Dust 4 on pressure surface	DUST4_ON_ISOBARIC_LVL	MASSMR
Dust 5 on pressure surface	DUST5_ON_ISOBARIC_LVL	MASSMR
Equilibrium level height	HGT_ON_EQUIL_LVL	HGT
Lightning	LTNG_ON_SURFACE	LTNG
Goes west channel 2 brightness Temperature	SBT112_ON_TOP_OF_ATMOS	SBT112
Goes west channel 3 brightness Temperature	SBT113_ON_TOP_OF_ATMOS	SBT113
Goes west channel 4 brightness Temperature	SBT114_ON_TOP_OF_ATMOS	SBT114
Goes west channel 5 brightness Temperature	SBT115_ON_TOP_OF_ATMOS	SBT115
In flight icing from NCAR algorithm	ICIP_ON_ISOBARIC_SFC	ICIP
Specific humidity at flight levels	SPFH_ON_SPEC_ALT_ABOVE_MEAN_SEA_LVL	SPFH
Virtual temperature based convective available potential energy	VTCAPE_ON_SURFACE	CAPE
Virtual temperature based convective inhibition	VTCIN_ON_SURFACE	CIN
Virtual temperature on model surfaces	Not currently available for grib2	NA
Virtual temperature on pressure surfaces	Not currently available for grib2	NA
Virtual temperature on flight levels	Not currently available for grib2	NA
Ventilation rate	VRATE_ON_PLANETARY_BOUND_LYR	VRATE
Haines index	HINDEX_ON_SURFACE	HINDEX
Pressure at flight levels	PRES_ON_SPEC_ALT_ABOVE_MEAN_SEA_LVL	PRES
Time-averaged percentage snow cover	AVE_SNOWC_ON_SURFACE	SNOWC
Time-averaged surface pressure	AVE_PRES_ON_SURFACE	PRES
Time-averaged 10m temperature	AVE_TMP_ON_SPEC_HGT_LVL_ABOVE_GRND_10m	TMP
Time-averaged mass exchange coefficient	AVE_AKHS_ON_SURFACE	AKHS
Time-averaged wind exchange coefficient	AVE_AKMS_ON_SURFACE	AKMS
Temperature at 10m	TMP_ON_SPEC_HGT_LVL_ABOVE_GRND_10m	TMP
Maximum U-component wind at 10m	MAX_MAXUW_ON_SPEC_HGT_LVL_ABOVE_GRND_10m	MAXUW
Maximum V-component wind at 10m	MAX_MAXVW_ON_SPEC_HGT_LVL_ABOVE_GRND_10m	MAXVW
Simulated GOES 12 channel 2 brightness temperature with satellite angle correction	NON_NADIR_SBT122_ON_TOP_OF_ATMOS	SBT122

Simulated GOES 12 channel 3 brightness temperature with satellite angle correction	NON_NADIR_SBT123_ON_TOP_OF_ATMOS	SBT123
Simulated GOES 12 channel 4 brightness temperature with satellite angle correction	NON_NADIR_SBT124_ON_TOP_OF_ATMOS	SBT124
Simulated GOES 12 channel 5 brightness temperature with satellite angle correction	NON_NADIR_SBT126_ON_TOP_OF_ATMOS	SBT126
Simulated GOES 11 channel 2 brightness temperature with satellite angle correction	SBT112_ON_TOP_OF_ATMOS	SBT112
Simulated GOES 11 channel 3 brightness temperature with satellite angle correction	SBT113_ON_TOP_OF_ATMOS	SBT113
Simulated GOES 11 channel 4 brightness temperature with satellite angle correction	SBT114_ON_TOP_OF_ATMOS	SBT114
Simulated GOES 11 channel 5 brightness temperature with satellite angle correction	SBT115_ON_TOP_OF_ATMOS	SBT115
Simulated GOES 15 channel 5 brightness temperature with satellite angle correction	Not currently available for grib2	NA
Simulated GOES 13 channel 2 brightness temperature with satellite angle correction	Not currently available for grib2	NA
Simulated AMSR-E channel 9 brightness temperature	AMSRE9_ON_TOP_OF_ATMOS	AMSRE9
Simulated AMSR-E channel 10 brightness temperature	AMSRE10_ON_TOP_OF_ATMOS	AMSRE10
Simulated AMSR-E channel 11 brightness temperature	AMSRE11_ON_TOP_OF_ATMOS	AMSRE11
Simulated AMSR-E channel 12 brightness temperature	AMSRE12_ON_TOP_OF_ATMOS	AMSRE12
SSMI F13 (19H 19V 37H 37V 85H 85V)	Not currently available for grib2	NA
SSMI F14 (19H 19V 37H 37V 85H 85V)	Not currently available for grib2	NA
SSMI F15 (19H 19V 37H 37V 85H 85V)	Not currently available for grib2	NA
SSMIS F16 (183H 19H 19V 37H 37V 91H 91V)	Not currently available for grib2	NA
SSMIS F17 (183H 19H 19V 37H 37V 91H 91V)	Not currently available for grib2	NA
SSMIS F18 (183H 19H 19V 37H 37V 91H 91V)	Not currently available for grib2	NA
SSMIS F19 (183H 19H 19V 37H 37V 91H 91V)	Not currently available for grib2	NA
SSMIS F20 (183H 19H 19V 37H 37V 91H 91V)	Not currently available for grib2	NA
MTSAT-1r imager channels 1-4 (backup for mtsat2)	Not currently available for grib2	NA

MTSAT2 imager channels 1-4	Not currently available for grib2	NA
Seviri brightness temperature channels 5-11	Not currently available for grib2	NA
Insat 3d brightness temperature IR channels 1-4	Not currently available for grib2	NA